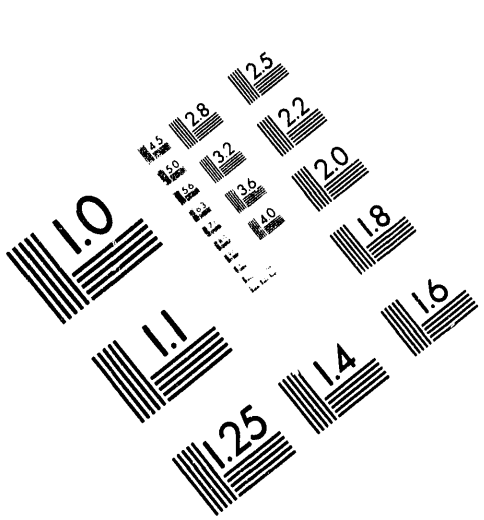

AIIM

Association for Information and Image Management
1100 Wayne Avenue, Suite 1100
Silver Spring, Maryland 20910
301/587-8202

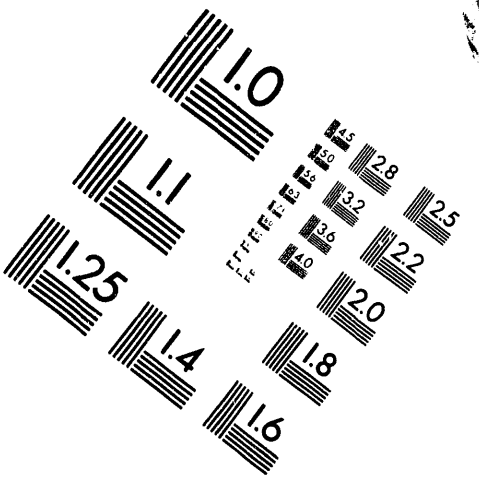

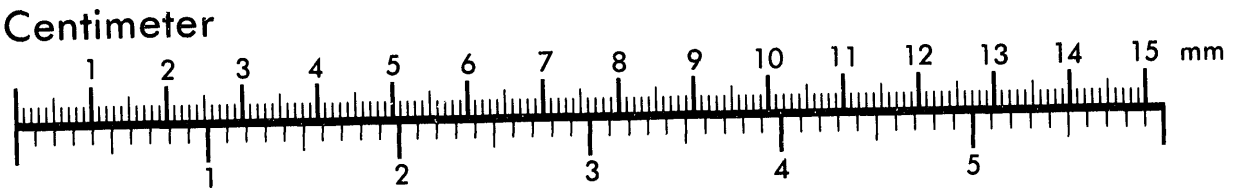

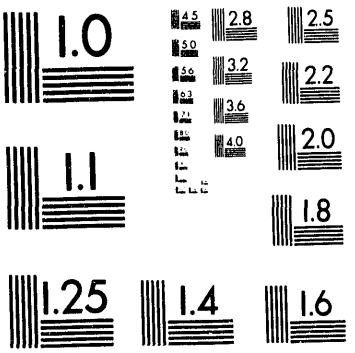

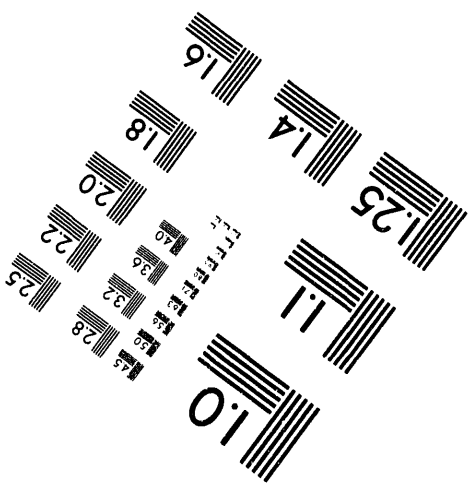

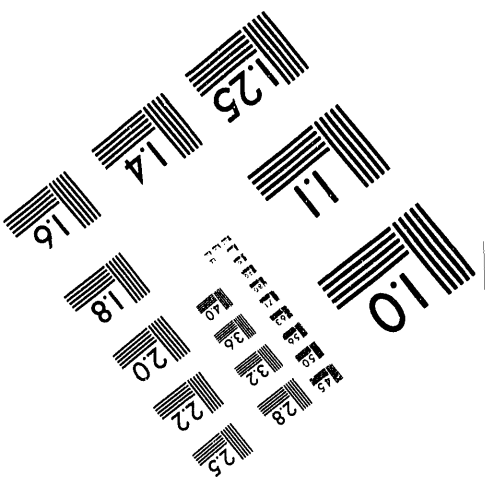

MANUFACTURED TO AIIM STANDARDS
BY APPLIED IMAGE, INC.

1 of 1

Conf-930695--1

David K.M. Shum[1]

INTERPRETATION OF WARM PRESTRESS-INDUCED FRACTURE TOUGHNESS BASED ON CRACK-TIP CONSTRAINT

REFERENCE: Shum, D.K.M., "**Interpretation of Warm Prestress-Induced Fracture Toughness Based on Crack-Tip Constraint,**" Fracture Mechanics: 25th volume, ASTM STP 1220, F. Erdogan and Ronald J. Hartranft, Eds., American Society for Testing and Materials, Philadelphia, 1994.

ABSTRACT: This study explores the possibility of using J-Q-related crack-tip constraint concepts to provide a basis for both the interpretation of warm prestress (WPS)-induced fracture toughness and their transferability to structural applications. A finite-element boundary-layer formulation based on small-scale yielding (SSY), remote mode I K-dominant assumptions is adopted. Effects of WPS-induced crack-tip constraint are quantified in terms of deviation in either the opening-mode or the mean stress component of the WPS crack-tip fields relative to the reference K-dominant SSY state associated with monotonic-loading conditions. Over the range of WPS load-paths considered the WPS-induced crack-tip constraint closely resembles a spatially varying hydrostatic stress field. Interpretation and transferability of WPS fracture toughness under SSY conditions are specified in terms of the unload and reload ratio.

KEYWORDS: warm prestress, J-Q theory, crack-tip constraint, fracture toughness, crack-tip fields, small-scale yielding

---

INTRODUCTION

Objective and Motivation

This paper describes preliminary findings from a study that explores the possibility of using J-Q-related crack-tip constraint concepts to provide a basis for both the interpretation of warm prestress (WPS)-induced fracture toughness and their transferability to structural applications [1]. Load-paths under WPS conditions are often non-monotonic in nature. Under monotonic-loading conditions, J-Q theory has been used to provide an explanation for the apparent specimen-geometry dependence of fracture toughness based on the associated variability in crack-tip constraint [2]. The objective of this study is to ascertain whether WPS-induced fracture toughness are likewise

---

[1]Development Staff, Oak Ridge National Laboratory, P.O. Box 2009, Oak Ridge, TN, USA 37831-8056

amendable to a J-Q-like explanation based on consideration of crack-tip constraint under WPS conditions.

Characteristics of Warm Prestress

In Fig. 1, the three types of warm prestress (WPS) benefits in relation to crack initiation are schematically illustrated. Type I: The mode I stress intensity factor (K_I) does not increase with time ($\dot{K}_I \leq 0$) after loading to K_{WPS}. Type-I WPS can be further specified in terms of neutral loading ($\dot{K}_I = 0$) or unloading ($\dot{K}_I < 0$) conditions. Crack initiation does not take place even if K_I and the crack-tip temperature are decreasing together such that the current value of K_I becomes greater than the fracture toughness for monotonically increasing loads (K_{Ic}). Type II: This type of WPS loading histories involves final reload to fracture from values of $K_I < K_{Ic}$. There is an apparent increase in fracture toughness upon reload (magnitude of K_I at failure = K_f) due to prior loading to K_{WPS} (above K_{IC} for the crack-initiation temperature) at a higher temperature such that $K_f/K_{Ic} \geq 1$. Type III: This type of WPS loading histories involves final reload to fracture from values of $K_I > K_{Ic}$ such that $K_f/K_{Ic} > 1$. It is emphasized that available experimental results on WPS-induced toughness enhancement are limited to mode I, quasi-static, plane strain, cleavage crack-initiation toughness values [1]. A significant obstacle in the way of including WPS effects in fracture-margin assessment is the need to use many global parameters to describe the WPS load history and, in the case of type-II and type-III WPS, the WPS-induced fracture toughness.

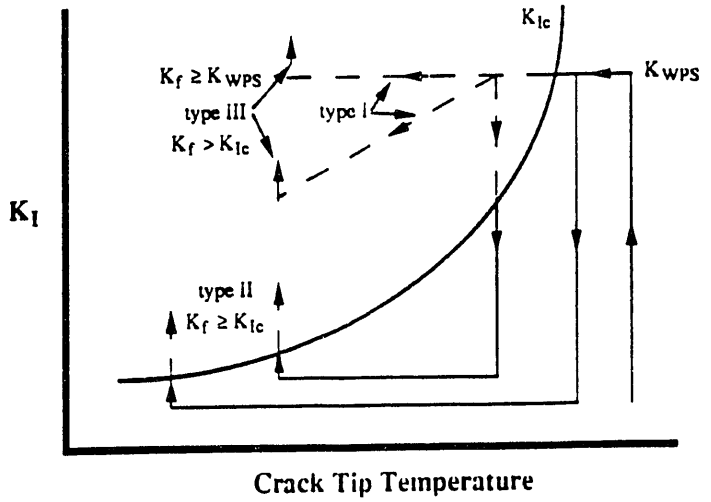

FIG. 1--Schematic illustrating three types of WPS benefits.

Regulatory Issues

Findings from a comprehensive literature survey on the phenomenon of WPS and its relation to regulatory issues relating to the operation of nuclear reactor pressure vessels (RPVs) are presented in Refs. [1,3]. An example regulatory issue that could potentially benefit from the findings of this study concerns the probabilistic analysis procedures used to evaluate the conditional probability of vessel failure [P(F|E)] under postulated pressurized-thermal-shock (PTS) accident conditions.

Current methodology for the evaluation of P(F|E) does not permit consideration of the potential benefits from WPS, in that crack initiation (and re-initiation subsequent to crack arrest) are assumed to take place when K_I exceeds K_{Ic} during the transient, regardless of the history of K_I as a function of transient time up to $K_I = K_{Ic}$ [4]. However, as indicated in Fig. 2, there is a wide range of analysis conditions during a PTS transient for which K_I first exceeds K_{Ic} at a time when K_I is decreasing with transient time. (In Fig. 2, decreasing crack-tip temperature corresponds to increasing transient time.) Inclusion of type-I WPS effects would imply that crack initiation would not take place under these conditions. Furthermore, potential benefits from considering type-II or type-III WPS effects would arise in cases where K_I increases with time after passing previous maximum and local minimum values during a transient. An example of this scenario is a PTS transient with re-pressurization.

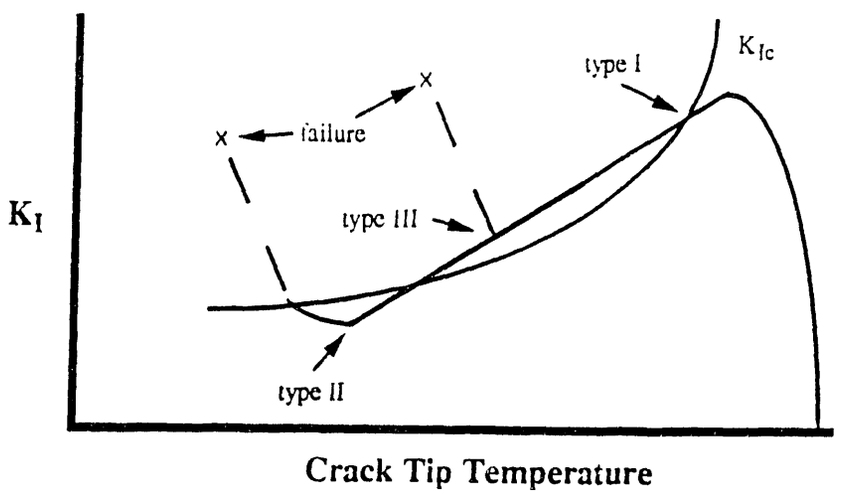

FIG. 2--Schematic illustrating range of crack-tip temperatures during a PTS transient for which inclusion of WPS effects would reduce P(F|E).

Status

Currently, the scarcity of information on the effects of WPS-related loading, unloading and reloading on the crack-tip fields in either small-scale specimens or anticipated vessel applications represents a significant obstacle in the way of inclusion of WPS effects toward the fracture-margin assessment of RPVs. Preliminary efforts toward addressing this obstacle via direct evaluation of the WPS-induced crack-tip fields in specimen and vessel geometries are presented in Ref. [1]. However, it is emphasized that while results on the WPS-induced crack-tip fields are becoming available, there is as yet no generally accepted basis for interpreting the results for the purpose of establishing the transferability of small specimen WPS-induced toughness data to vessel applications.

FINITE ELEMENT ANALYSIS FORMULATION

A finite-element-based, small-scale yielding (SSY), boundary-layer (BL) formulation is employed as the framework for this study [1]. A SSY-BL formulation provides a general means to study the interaction between geometry (small-scale specimen or structure) and loading (thermal and/or mechanical) effects on crack-tip fields without the complexity of a case by case geometry- and load-specific evaluation. Conditions of SSY are naturally incorporated into a BL analysis via the imposition of appropriate "remote" boundary conditions. To the extent that SSY conditions exist in small-scale specimens and vessel applications subjected to WPS loading, the results from this development effort serve to establish an analytical basis for transferability.

Focus

The phenomenon of WPS loading and hence WPS-induced fracture toughness is anticipated to be a consequence of the combined influences of load-path and/or temperature-dependent material properties on the micromechanics of fracture. The emphasis of this study is on investigating the influence of load-path (stress and strain loading histories) on the crack-tip fields and, by extension, the propensity for crack initiation. The temperature-dependence of material stress-strain relation is not considered. The *isothermal* results to be presented are thus applicable to WPS loading situations in which the WPS-induced stress and strain loading histories represent the primary factors that influence the onset of crack initiation. In this sense, the effects of the WPS temperature excursion on a material's stress-strain relation, and indirectly on the tendency for crack initiation, are considered secondary effects.

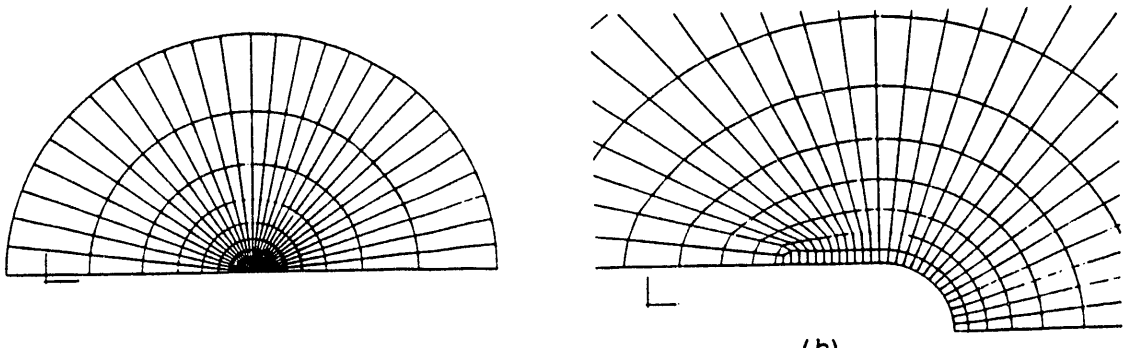

(*a*) (*b*)

FIG. 3--Finite element model of SSY-BL formulation. (*a*) Global model. (*b*) Close-up of near-crack-tip region.

Finite Element Model

In the present finite-element-based boundary-layer approach, the near-crack-tip region over which the crack-tip-opening displacement (CTOD or δ) sets the size-scale of the problem is modeled by constructing a finite-element mesh with a suitably large outer boundary as indicated in Fig. 3(*a*). A unique feature of the finite-element mesh is the highly refined crack-tip region and the assumption of an initial root radius prior to the imposition of external loading as indicated in Fig. 3(*b*). The outer radius of the mesh in Fig. 3(*a*) is ~1×10^6 times the initial root radius indicated in Fig. 3(*b*). The finite-element mesh

in Figs. 3(*a*,*b*) is made up of 1119 8-node, isoparametric plane-strain elements and 3492 nodes. The integration order of these elements is 2x2.

Material Properties

Uniaxial stress-strain results for an unirradiated A533B steel at 177°C (350°F), taken from a steel plate designated as HSST plate 13-A, are used to construct the reference stress-strain curve employed in the analyses [5]. The true stress-true plastic strain curve normalized with respect to the yield stress is indicated in Fig. 4. The material properties are as follows: Young's Modulus (E) = 197 GPa (28600 ksi), Poisson's ratio (ν) = 0.3, initial yield stress (σ_o) = 390 MPa (56.6 ksi), and ultimate stress (σ_u) = 613 MPa (88.9 ksi). Selection of the stress-strain curve indicated in Fig. 4 is motivated in part by the WPS fracture toughness results for unirradiated A533B steel described in Ref. [6], where the WPS preload is carried out at 177°C. Since the emphasis of this investigation is on isolating the influence of WPS-induced stress and strain loading histories on the crack-tip fields, temperature-dependence of the uniaxial stress-strain curve is not considered.

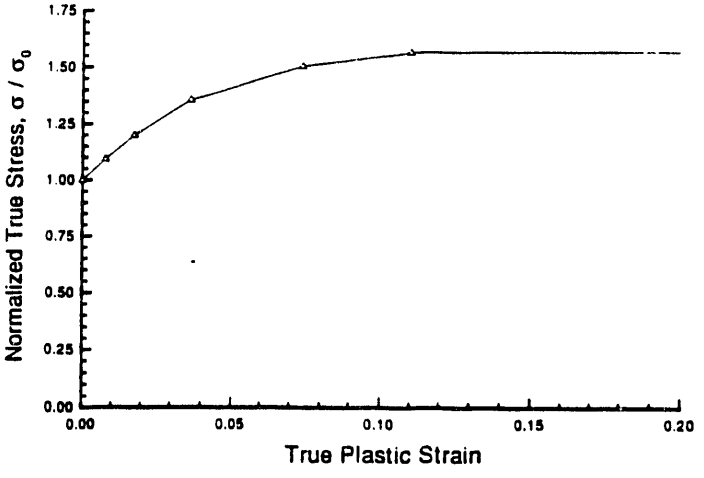

FIG. 4--Uniaxial true stress-true plastic strain curve.

Loading Conditions and Analysis Assumptions

Attention is focussed on quantifying the mode I plane strain near-tip crack-tip fields under isothermal, K-dominant far-field conditions. Three single-cycle load-paths that correspond to:

(1) load-partial-unload-reload (LPUR) with 1/3 unloading,
(2) LPUR with 2/3 unloading, and
(3) load-unload-reload (LUR) with full unloading,

are considered. In all cases considered herein, the maximum value of the remote mode I stress intensity factor (K) upon reload is identical to the value of the remote K at initial loading. The K-dominant far-field conditions are applied as displacement boundary conditions on the outer-boundary of the finite element mesh. The conditions of SSY require that the spread of plasticity be confined within the elastic "far-field" of the finite-element mesh. In this study, this SSY requirement is accomplished by limiting the maximum extent of the plastic zone to be <10% of the outer mesh dimension. Value of the CTOD

upon reaching the initial K value is >10 times the initial notch opening so that self-similarity of the SSY results under the initial monotonic preload is guaranteed. A rate-independent, large-deformation, J_2 (isotropic-hardening) incremental plasticity theory is adopted in evaluating the near-tip crack-tip fields [7]. Limited data on the cyclic uniaxial response of the material from steel plate 13-A suggest that the above material formulation is appropriate for this phase of the investigation [1].

Crack-Tip Characterization Based on Remote Value of J-Integral

For a stationary crack under monotonically increasing mode I plane strain K-dominant SSY conditions, value of the remotely applied K provides both a measure of the crack-driving force and a convenient length-scale [in terms of $(K/\sigma_o)^2$] with which to normalize the near-tip fields into self-similar distributions. Identification of the J-integral (J) as either (1) the energy-release rate, or (2) the amplitude of the elastic-plastic crack-tip fields, under these conditions provides alternate measures of the crack-driving force in terms of J. The equivalence of J based on these two methods of evaluation is ensured since J is path independent under these conditions. Identification of J as a crack-tip-field amplitude parameter also serves to uniquely characterize the elastic-plastic near-crack-tip fields in the form of self-similar distributions based on the length-scale J/σ_o.

However, consideration of WPS necessarily involves non-monotonic load-paths that result in unloading and reloading of the crack tip region. Within the context of a SSY-BL framework with the requisite remote elastic region, the value of the "remotely" applied K remains uniquely defined throughout a given load-cycle. Consequently, characterization of the crack-driving force in terms of a "remote" value of J remains possible. On the other hand, the relation between the "remote" value of J and features of the elastic-plastic crack-tip fields are undetermined. That is, the potential for the near-tip deformation level to be characterized by a J-related parameter alone remains an open issue. Nevertheless, partly in deference to fracture mechanics concepts developed for monotonic-loading conditions, the remote value of J in terms of J/σ_o is also used to provide the near-tip length-scale to scale the crack-tip deformation in this study. The near-tip elastic-plastic crack-tip fields thus determined are expected to be load-path dependent, such that in general the crack-tip fields cannot be uniquely related to the remotely applied value of K in the sense of a self-similar distribution. One outcome of this study is the quantification of this path dependence, and a preliminary determination of the appropriateness of using the remote value of J to thus scale the non-monotonic near-tip crack-tip fields.

FINITE ELEMENT ANALYSIS RESULTS

The nomenclature K_{WPS} is adopted herein to facilitate identification of the magnitude of the initial preload in the analyses with the prior load-cycle associated with WPS loading. Subsequent load-paths are expressed *relative* to this initial value. It is emphasized that the results presented herein are general in nature in that they are not dependent on the specific value of K_{WPS} or the specific values of K during unloading or reloading. Rather, the requirements of SSY

conditions are such that the results are dependent only on the value of K *relative* to K_{WPS}. Within the present single-parameter methodology, unloading is characterized by the *unload ratio* $\Delta K/K_{WPS}$, while reloading is characterized by the *reload ratio* K/K_{WPS}.

J-CTOD Relations

Relations between the remote value of J and CTOD (δ) as a function of load-paths are indicated in Fig. 5. The applied load is expressed in the normalized form $(J/\sigma_o)/\delta_o$, where δ_o is the initial notch opening prior to loading. The CTOD is also normalized with respect to δ_o. In Fig. 5, results are indicated for the following load-paths:

(1) Monotonic loading from the initial unloaded state to target value K_{WPS}.
(2) Monotonic unloading from K_{WPS} to unloaded state (full unloading, $\Delta K/K_{WPS} \leq 1$).
(3) Monotonic reloading from the 2/3 K_{WPS} point on the unloading line to K_{WPS} (1/3 unloading, $\Delta K/K_{WPS} = 1/3$, $2/3 \leq K/K_{WPS} \leq 1$).
(4) Monotonic reloading from the 1/3 K_{WPS} point on the unloading line to K_{WPS} (2/3 unloading, $\Delta K/K_{WPS} = 2/3$, $1/3 \leq K/K_{WPS} \leq 1$).
(5) Monotonic reloading from the unloaded state to K_{WPS} (full unloading, $\Delta K/K_{WPS} = 1$, $0 \leq K/K_{WPS} \leq 1$).

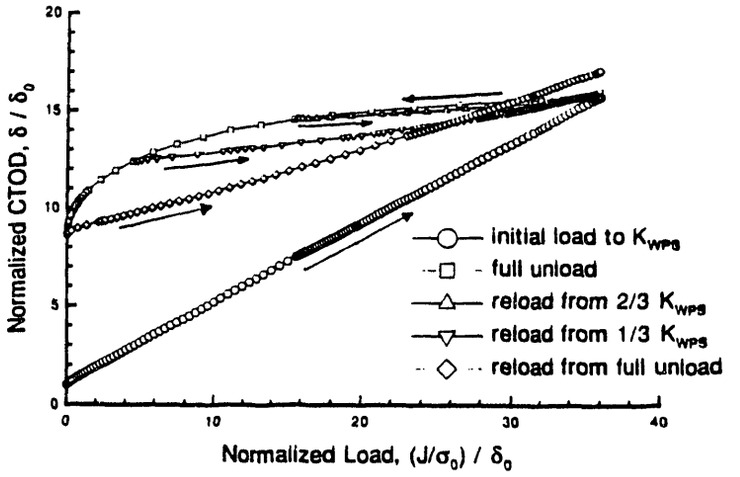

FIG. 5--Relations between remote value of J and CTOD (δ) as a function of load-paths for values of K under reloading up to K_{WPS}.

Crack-Tip Fields During Unloading

Distributions of the opening-mode stress component (σ) during various stages of unloading are indicated in Fig. 6(a) as a function of the original undeformed distances ahead of the crack tip along the crack plane. The opening-mode stress is normalized with respect to σ_o, while distances ahead of the crack tip are normalized with respect to the current value of J/σ_o. It is emphasized that the value of J/σ_o is obtained based on the remote value of $(K/\sigma_o)^2$, and is therefore a length-scale based on global and not near-tip considerations. The results in Fig. 6(a) include a range of unloading down to ~55% K_{WPS}. The curve denoted as "SSY" represents the distribution associated with

the initial monotonically applied load-cycle at K_{WPS}, such that the SSY curve represents the theoretical self-similar K-dominant distribution for the material under monotonic-loading conditions.

Deviations (differences) of the unloading results from the reference SSY distribution are made explicit in Fig. 6(*b*), where these deviations are expressed in terms of differences in σ between the unloading results and the SSY distribution. Numerical results for these deviations expressed alternatively in terms of differences in the mean (hydrostatic) stress σ_m can be found in Ref. [1]. Results shown in Fig. 6(*b*) and similar plots to be presented will be used to provide quantitative and qualitative measures of WPS-induced crack-tip constraint in a manner to be explained shortly.

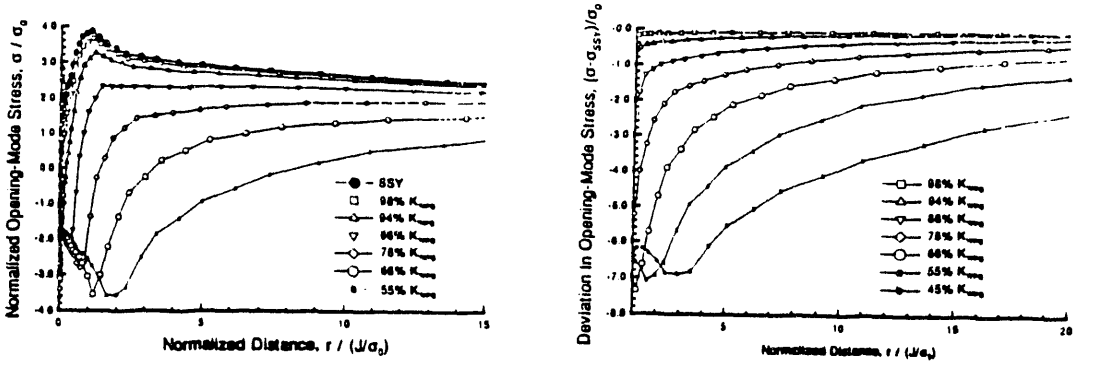

(*a*) (*b*)

FIG. 6--(*a*) Distributions of σ along the crack plane directly ahead of the crack tip for a range of unloading down to ~55% K_{WPS}. Also indicated is the SSY distribution. (*b*) Deviations of the unloading results from the SSY distribution in terms of σ.

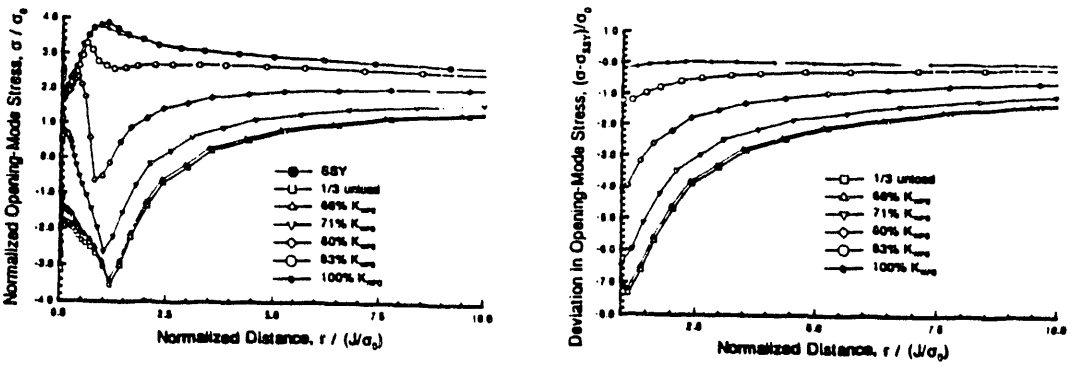

(*a*) (*b*)

FIG. 7--(*a*) Distributions of σ during various stages of reload from 2/3 K_{WPS} after 1/3 unloading. Also indicated is the distribution at the end of the 1/3 unload cycle. (*b*) Deviations of the reload from 2/3 K_{WPS} results from the SSY distribution in terms of σ.

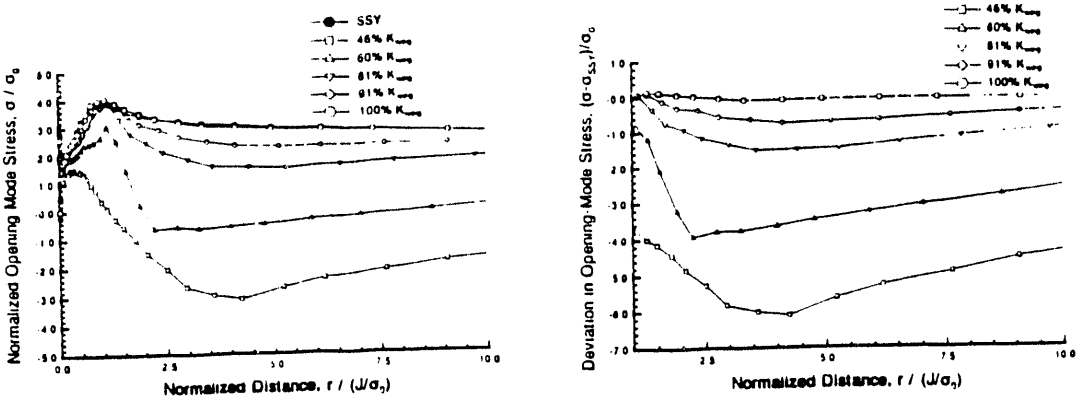

(*a*) (*b*)

FIG. 8--(*a*) Distributions of σ during various stages of reload from 1/3 K_{WPS} after 2/3 unloading. (*b*) Deviations of the reload from 1/3 K_{WPS} results from the SSY distribution in terms of σ.

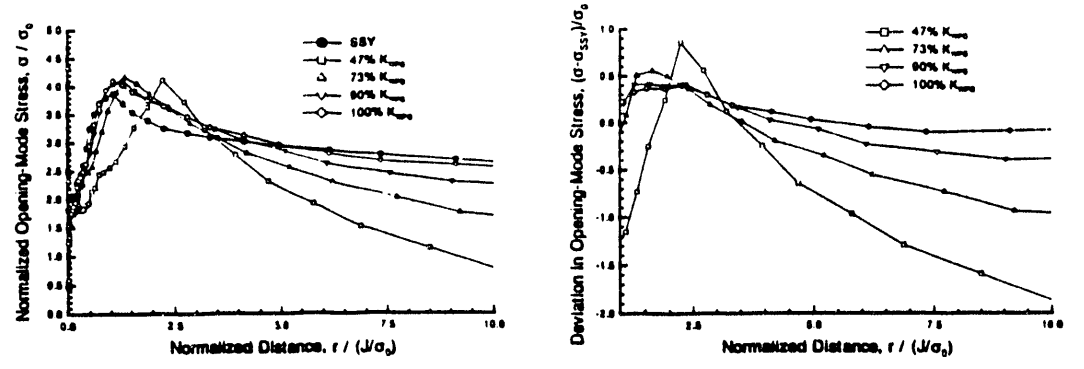

(*a*) (*b*)

FIG. 9--(*a*) Distributions of σ upon reload up to K_{WPS} after full unloading. (*b*) Deviations of the reload from full unload results from the SSY distribution in terms of σ.

Crack-Tip Fields During Reload After Unloading

Distributions of σ, during various stages of reload from 2/3 K_{WPS} after 1/3 unloading, are indicated in Fig. 7(*a*). The curve denoted as "1/3 unload" represents the distribution associated with the end of the 1/3 unload-cycle with unload ratio $\Delta K/K_{WPS}$ ~1/3. The curve denoted as "66%" represents the distribution at the onset of the reload-cycle with reload ratio K/K_{WPS} ~66%. The curve denoted as "100%" represents the distribution at the end of the reload-cycle with reload ratio K/K_{WPS} = 1. The "1/3 unload" and "66%" curves are shown together to indicate the essential "continuity" of crack-tip fields immediately prior to and after reloading. A similar degree of "continuity" of crack-tip fields is observed after 2/3 and full prior unload. Consequently, the "unloaded" distribution of crack-tip fields associated with 2/3 unload and full unload are not shown in subsequent figures. Distributions of σ, during various stages of reload from 1/3 K_{WPS} after 2/3 unloading ($\Delta K/K_{WPS}$ ~2/3), are indicated in Fig. 8(*a*). Distributions of σ upon reload after full unloading are indicated in Fig. 9(*a*). In Figs. 7(*b*), 8(*b*) and 9(*b*), deviations of the reload results from the reference SSY

distribution in terms of differences in σ, at various stages of reload after 1/3, 2/3 and full unloading, are presented.

INTERPRETATION OF NEAR-TIP CRACK-TIP FIELDS

Results in Figs. 6 to 9 confirm the expectation that under non-monotonic loading conditions the near-tip crack-tip fields are load-path dependent and cannot be uniquely related to the remotely applied value of K. That is, the unloading and reloading near-tip crack-tip fields do not exhibit the self-similar spatial distribution (denoted as SSY in the figures) that exists under monotonic-loading conditions. It is emphasized that the conformance to the *elastic*, monotonic K-dominant distribution increases with increasing distance from the crack tip, and that the conformance becomes exact as the outer boundary of the finite element mesh is approached.

Monotonic Unloading With Unload Ratio $\Delta K/K_{WPS} \leq 1$

Analysis results in Figs. 6(*a*,*b*) indicate that under monotonic-unloading ($\dot{K}_I < 0$) type-I WPS conditions the crack-tip constraint state is relaxed relative to the reference (K-dominant SSY) state that exists prior to the onset of unloading. With reference to Figs. 6(*a*,*b*), the following observations are made:

(1) The loss of crack-tip constraint exhibits some degree of spatial dependence.
(2) Both the magnitude and the spatial dependence of the constraint loss increase with increasing unloading as quantified by the value of $\Delta K/K_{WPS}$.
(3) The spatial dependence of the constraint loss is monotonic with respect to distances ahead of the crack tip for unload ratios $\Delta K/K_{WPS} \geq 2/3$.

As discussed in Ref. [1], it is also observed that the loss of crack-tip constraint closely resembles a spatially varying hydrostatic stress field due to the near equivalence in the calculated deviations in terms of σ and σ_m, and that the magnitude of the constraint loss is greater based on σ than σ_m.

One traditional explanation for the effects of monotonic-unloading type-I WPS is attributed to the progressive formation of residual compressive zones around the crack tip which provide "crack closure" forces that inhibit crack initiation [1]. The progressive formation of residual compressive zones around the crack-tip region during unloading is confirmed by the isothermal results in Fig. 6(*a*), where negative values of σ are indicative of the extent of the residual compressive zone. On the other hand, the results in Figs. 6(*a*,*b*) are also suggestive of an alternate explanation for the absence of crack initiation under monotonic-unloading type-I WPS conditions. Specifically, the crack-tip field results presented here suggest a correlation between the extent of monotonic unloading and the loss of crack-tip constraint. Based only on the results presented here, however, it is not possible to determine if the observation of no crack initiation with decreasing K_I (and K_{Ic}) values is a *consequence* of the associated loss of constraint, or if the evident loss of constraint with unloading is merely a manifestation of the phenomenon of unloading. That is, the present observation of a correlation does not rule out the possibility that crack initiation does not take place under type-I WPS

due to the intervention of physical postulates that are not captured by the stress analysis. However, it is emphasized that since type-I WPS does not involve consideration of *toughness enhancement per se* (no initiation), understanding the potential relationship between crack-tip constraint and type-I WPS is not a necessary precursor to making use of the beneficial effects of type-I WPS.

Reload From Unload Ratio $\Delta K/K_{WPS} = 1/3$

Results in Figs. 7(*a*,*b*) indicate that with 1/3 prior unload, the crack-tip constraint state remains relaxed relative to the reference K-dominant SSY state up to a reload ratio of $K/K_{WPS} = 1$. The crack-tip fields at a given value of the reload ratio K/K_{WPS} are, as expected, load-path dependent. With reference to Figs. 7(*a*,*b*), observations #1 and #2 for the $\Delta K/K_{WPS} \leq 1$ results apply here also. Observation #3 is modified in that the spatial dependence of the constraint loss is monotonic with respect to distance ahead of the crack tip throughout the unload-reload cycle. With respect to observation #3, it is noted that the spatial distribution of the constraint loss under reload is very similar to that under unloading. In a manner somewhat similar to that observed for the monotonically unloading results discussed previously, the reload results suggest that effects of reload from limited prior unloading are likewise amenable to a constraint-based correlation or description.

Reload From Unload Ratio $\Delta K/K_{WPS} = 2/3$

Results in Figs. 8(*a*,*b*) indicate that with 2/3 prior unload, observations #1 and #2 reported for the 1/3 prior unload results continue to apply in the present case. Specifically, constraint relaxation is observed up to a reload ratio of $0.91 < K/K_{WPS} < 1$. The observed increase in constraint for $K/K_{WPS} = 1$ is minimal. On the other hand, the spatial dependence of the constraint loss is non-monotonic with respect to distances ahead of the crack tip throughout the unload-reload cycle.

Reload From Unload Ratio $\Delta K/K_{WPS} = 1$

Results in Figs. 9(*a*,*b*) indicate that the nature of the near-tip crack-tip fields, and hence the character of the crack-tip constraint, are very different for the present case of $\Delta K/K_{WPS} = 1$ as compared with $\Delta K/K_{WPS} = 1/3$ or 2/3. Furthermore, the relative increase or decrease in crack-tip constraint is dependent on the location ahead of the crack tip, in addition to the value of the reload ratio K/K_{WPS}. For the range of reload ratios indicated, the crack-tip constraint over the approximate region $1 \leq r/(J/\sigma_o) \leq 3$ is higher than the reference K-dominant SSY condition. The observation of higher crack-tip constraint is significant since it suggests the possibility of *anti-shielding* of the crack-tip and hence toughness degradation under certain range of WPS conditions and will be addressed in a latter section.

Numerical results in Ref. [1] indicate that constraint deviation from the SSY state for the case of full unload essentially disappears by reloading to $K_I \geq 1.6\ K_{WPS}$, which indicate that the combined effects of load-path dependence due to prior unloading and reloading on the crack-tip fields are "washed out" by ~1.6 K_{WPS}. The observation of

progressive return to the SSY constraint state with increasing reload is reflected by the progressive change in the slope of the J-CTOD results presented in Fig. 5. Based on the progressive evolution of crack-tip fields indicated in Figs. 7 and 8, a similar disappearance of constraint deviation before reaching 1.6 K_{WPS} is anticipated for the cases of 1/3 and 2/3 prior unload. The observation of conformance to SSY conditions suggest that potential effects of WPS loading on constraint, whether they be shielding or anti-shielding in nature, only operate over a limited range of the loading conditions. It is possible to establish a qualitative connection between the *load-path* results presented thus far with crack-tip conditions associated with *fatigue* applications [8]. The load-path results provide a numerical justification for the suggestion that, when the range of fatigue cycling is limited with respect to the final fracture condition in terms of relative values of K, the cumulative effects of the prior cycling on the crack-tip conditions at the onset of crack initiation are insignificant.

Anti-Shielding Effects Under Warm Prestress Conditions

Experimentally, conditions of WPS are associated with toughness enhancement. Recent studies in the area of crack-tip constraint suggest that the loss of crack-tip constraint represents one avenue through which toughness enhancement can be achieved under monotonic-loading conditions [2,9]. Consequently, the observation of increase in crack-tip constraint, and hence the potential for anti-shielding or toughness degradation effects, under a range of WPS-related load-unload-reload conditions is somewhat unexpected. It might be suggested that the prediction of constraint increase is indicative of errors associated with the SSY formulation presented here. The monotonic-loading results are consistent with available results in the open literature. Consequently, any potential errors within the current formulation are likely to be limited to the extent to which the assumed isotropic-hardening plasticity formulation can accurately capture the physical stress and strain response of RPV-grade steels under load-unload-reload conditions. Recall that the isotropic-hardening formulation is adopted based on rather limited experimental data. Further confirmation of the appropriateness of this choice awaits additional experiments to elucidate the cyclic-yielding behavior of RPV-grade steels.

The analysis assumption of a stationary crack has also been identified as a potential source of error within the present formulation [1]. Under conditions representative of those encountered in an RPV under PTS conditions, a *rough* estimate of the extent of crack blunting/growth due to a load-full unload cycle is ~0.14 J/σ_0. With reference to Figs. 9(*a* and *b*), it remains to be determined if a WPS crack-tip model that takes into account limited crack blunting/growth would exhibit anti-shielding effects.

On the other hand, an intriguing possibility is that the anti-shielding results do indeed capture the essential nature of the near-tip stress and strain distributions for an RPV-grade steel after one load-unload-reload cycle. Motivation for this viewpoint comes from the observation that the results can be viewed as qualitatively describing certain aspects of the so-called "zero to tension" full-unloading fatigue cycle [8]. Within a fatigue interpretation, the results presented here would suggest the possibility of a constraint-based element to the fatigue crack-growth process. However, it is emphasized that this viewpoint certainly requires additional confirmation. It is

recognized that differences exist between the present model of a stationary "sharp" crack and a steadily propagating crack associated with fatigue. For example, crack-closure is not observed in the present analysis results under full unloading (see Fig. 5) , while it is observed for a steadily propagating fatigue crack under full unloading [7].

IMPLICATIONS TOWARD TRANSFERABILITY

Analysis results presented thus far have quantified the nature of the crack-tip fields, within the assumptions of K-dominant SSY conditions, as a function of unload and reload ratios. Insofar as these results do not depend explicitly on geometry and loading conditions, these results provide a first step toward unifying the wide range of WPS loading conditions encountered in specimen and structural applications. It is emphasized that these results represent self-similar fields in that they are valid for the specified ratios of unloading and reloading, and are not dependent on the magnitude of individual K values themselves. In this section, the implications of these near-tip crack-tip fields toward the transferability of fracture toughness data under conditions of WPS will be addressed in light of transferability methodologies developed for monotonic-loading conditions.

Transferability Based on Global Conditions

Near-tip results presented thus far indicate that for a wide range of unload-reload conditions the near-tip fields are not uniquely related to the current value of the remote K. However, transferability based on similarity of the global crack-tip fields remains possible within the present SSY framework if the loading conditions are specified in terms of both the unload and reload ratios $\Delta K/K_{WPS}$ and K/K_{WPS}. That is, a unique correlation does exist between the near-tip crack-tip fields and the remote K-dominant annular region when the unload and reload histories of that annular region, and not simply the current value of K, are specified. The proposed history-dependent correlation is akin to the treatment of transferability of small-specimen fatigue data to structural applications based on various empirical fatigue correlations [8]. The strength of a transferability methodology based on "global" annular fields is that it does not involve explicit evaluation of the near-tip elastic-plastic crack-tip fields that more directly determine the fracture event. However, the empirical nature of this transferability methodology requires close "matching" of the global conditions associated with small-scale specimens and structural application. For example, a limitation of the SSY requirement is that small-specimen WPS toughness data generated under general-yielding conditions cannot be used to assess the fracture response of a structure under globally linear-elastic conditions.

Transferability Based on Near-Tip Conditions

In a manner analogous to K- and J-based approaches, the J-Q approach for monotonic loading permits a unique correlation between continuum crack-tip fields within a J-Q annulus and the stress and strain fields within the fracture process zone [2]. Within a J-Q approach and based on theoretical considerations, the J-integral provides the characteristic near-tip length-scale (via J/σ_0) that highlights the self-similar nature of the elastic-plastic crack-tip

fields as a function of crack-tip constraint relative to conditions of SSY. That is, when the spatial distributions of the crack-tip stress and strain fields are scaled with respect to the current value of J/σ_o, the resultant distributions permit the ordering and hence comparison of crack-tip constraint in a manner characteristic of the near-tip deformation states.

At present, there are no analogous theoretical considerations that establish the nature of the continuum elastic-plastic crack-tip fields under non-monotonic loading conditions. For this reason, it was emphasized previously that the current value of J/σ_o merely represents a convenient length-scale by which to normalize the non-monotonic near-tip results, and that the relation between the current value of J/σ_o and the nature of the near-tip deformation is undetermined. Indeed, the analysis results presented here represent a first attempt at a detailed numerical description of the non-monotonic crack-tip fields. Consequently, work remains to develop an alternate approach to the establishment of transferability based on near-tip length-scales that can characterize the nature of the elastic-plastic crack-tip deformation under non-monotonic loading conditions. An example of the type of approach that might be needed can be found in the development of the length-scale L_g associated with the characterization of near-tip crack-tip fields under steady-state mode I crack growth conditions [10]. The main advantage of a near-tip approach, should its development prove successful, is to eliminate the limitation that small-specimen WPS toughness data must be generated under SSY conditions for applications to structural scenarios involving globally linear-elastic conditions.

Relation to Monotonic-Loading J-Q Constraint Concepts

Within a SSY formulation, Q-stress constraint effects under monotonic-loading conditions are the consequence of non-zero values of the remote T-stress. On the other hand, the constraint effects under non-monotonic loading conditions discussed herein are entirely a consequence of load-path effects and not attributable to the T-stress since T = 0 in this study. The absence of a theoretical framework for organizing the non-monotonic near-tip results is the major reason why J-Q constraint concepts developed for monotonic-loading conditions strictly cannot be applied in this case. Nevertheless, a number of similarities in the crack-tip fields are evident between these two sets of conditions. Consequently, the question remains concerning the extent to which these two types of constraint effects can be treated within a unified framework. Comprehensive answers to these questions are not available at this time. Instead, a number of observations based on a *formal* (ie, without theoretical rigor) interpretation of the non-monotonic results within the J-Q approach are offered for future considerations.

According to the J-Q approach, the loss of crack-tip constraint is quantified based on evaluation of the difference-field associated with a given application. Specifically, the constraint parameters Q and Q_m (based on σ and σ_m respectively) are defined at crack-tip location $r = 2 J/\sigma_o$. The appropriateness of the J-Q characterization is determined based on the gradient parameters Q' and Q_m' satisfying the inequalities $Q' \leq 0.1$ and $Q_m' \leq 0.1$ [2]. One avenue to illustrate the effects of prior unloading on crack-tip constraint under reloading conditions is to follow the formalism of the J-Q methodology. Specifically, Q-like and

Q_m-like parameters are evaluated based on the stress distributions indicated in Figs. 7(b), 8(b) and 9(b). The results of this formal evaluation are presented in Fig. 10 as a function of the extent of prior unloading ($\Delta K/K_{WPS}$) and the magnitude of the reload ratio K/K_{WPS}. In Fig. 10, the vertical axis is labelled as indicated to emphasize the manner in which the constraint parameters are evaluated without explicit identification with either Q or Q_m. However, it is of interest to note that for the case of 1/3 prior unload, the constraint-loss indicated in Fig. 10 can formally be phrased in terms of the Q and Q_m parameters for $K/K_{WPS} \geq 0.93$ based on satisfying the "validity" requirements pertaining to the gradient parameters Q' and Q_m'. For the case of 2/3 prior unload, a formal description based on Q and Q_m is possible for $K/K_{WPS} \geq 0.91$. For the case of full unload, a formal description based on Q and Q_m is possible for $K/K_{WPS} \geq 0.73$.

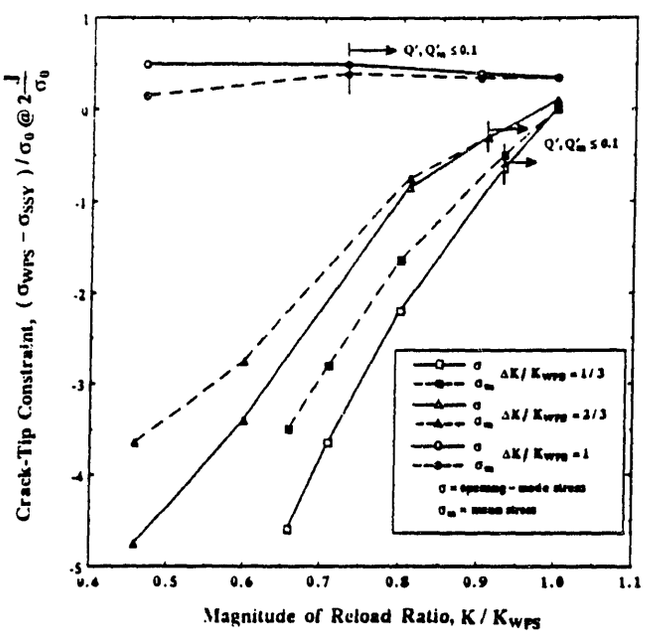

FIG. 10--Crack-tip constraint as a function of $\Delta K/K_{WPS}$ and K/K_{WPS}.

Notwithstanding the appropriateness of a Q- or Q_m-based description of the WPS-induced constraint loss, results in Fig. 10 indicate that for a given magnitude of the reload ratio K/K_{WPS}, constraint relaxation varies inversely with the extent of prior unloading. Therefore, to the extent that loss of constraint (in terms of σ or σ_m) can be correlated with a greater "resistance" to crack-initiation relative to the SSY state, these results are in qualitative agreement with the experimentally observed trend of decrease in WPS-induced toughness with increase in the amount of unloading during the WPS cycle [6]. However, the above constraint-based interpretation of unloading effects is in some sense fortuitous. It is observed from Figs. 7 to 9 that the nature of the difference-fields, in terms of their dependence on distances ahead of the crack tip, vary widely for the three cases considered. Furthermore, the spatial dependence is monotonic for the case of 1/3 prior unload but non-monotonic for the cases of 2/3 and full prior unloading. The nature of the constraint

deviation has also been quantified based on two other crack-tip locations, $r = 5\ J/\sigma_o$ and $r = 7\ J/\sigma_o$ [1]. In the latter two cases, when the results are presented in the form of Fig. 10, it is observed that the constraint loss is now slightly greater for 2/3 prior unloading than 1/3 prior unloading. However, the constraint loss for both 2/3 and 1/3 prior unloading remains substantially greater than that for the case of full unloading.

ADDITIONAL CONSIDERATIONS

Effects of Multiple Cycles

A comment on the practical utility of a constraint-based description of the effects of type-II and type-III WPS on crack-tip fields and fracture toughness is appropriate at this point. For the purpose of ease in illustration, it will prove convenient to phrase the comment within the context of a J-Q constraint approach. That is, it is assumed that the J-Q methodology provides a viable means to characterize the near-crack-tip fields (crack-driving force and crack-tip constraint) over certain ranges of the WPS load-path in terms of the load-trajectory J(Q) and hence a toughness locus expressible in terms of $J_c(Q)$. Potential limitations on the practical utility of the J-Q approach to WPS loading conditions exist if J(Q) and/or $J_c(Q)$, in addition to being depending on the load-path, are also dependent on the *number* of load-path cycles N such that J(Q,N) and $J_c(Q,N)$. Example RPV applications that potentially involve multiple-cycle WPS-type load-paths include the start-up/cool-down refueling cycles and PTS transients with thermal and pressure oscillations. Note that limited results for an A508 steel indicate that the WPS-induced toughness is independent of the number of WPS cycles [11]. Clearly, much experimental and analytical work remain toward resolving the impact of cyclic loading on a constraint-based description of WPS effects.

Effects of General Yielding

Within the present SSY formulation, the load-path has no effects on the crack-driving force since the crack-driving force is part of the specified boundary conditions. Instead, the effects of unloading and reloading are to shield the crack-tip via decrease in the crack-tip constraint relative to SSY conditions. However, it is conceivable that under general large-scale yielding conditions, unloading and reloading can shield the crack-tip by decreasing both the crack-tip constraint and the crack-driving force (or equivalently the deformation level). Consequently, as the nature of the near-tip fields under non-monotonic conditions are not known, the possibility of different shielding effects under small scale and general yielding provide another motivation for establishing transferability based on matching of global conditions.

Implications Toward Vessel Analysis

The WPS-induced crack-tip fields in an RPV subjected to a series of related PTS transients that include repressurization have recently become available [1]. An approximate but direct comparison between the K-dominant SSY and the RPV results indicate that the vessel WPS loading does indeed take place under near K-dominant SSY conditions. Consequently, the present SSY formulation can be used to model a variety

of PTS-related WPS loading conditions. A significant finding from the RPV analyses is that deviation of the RPV crack-tip fields from the reference K-dominant SSY conditions is significant only for transient times beyond the initial unloading of the crack tip. Consequently, inclusion of load-path effects on crack-tip constraint is indeed a necessary precursor to the application of constraint concepts (eg. J-Q) toward the fracture-margin assessment of RPVs under PTS conditions.

Implications Toward Interpretation of Small-Specimen Data

The crack-tip fields in small-scale specimens subjected to a complete WPS load cycle are not yet available. Preliminary analysis results for a 4T-planform compact-tension specimen geometry for which WPS experimental data are available indicate the presence of significant three-dimensional crack-tip constraint effects during the monotonic-loading phase of the WPS load cycle [1]. Consequently, inclusion of T-stress effects in the present SSY formulation is necessary toward a more realistic simulation of the small-specimen WPS-induced crack-tip fields.

CONCLUSIONS

Evaluation of load-path effects associated with monotonic unloading type-I WPS indicates progressive loss of crack-tip constraint with increase in the amount of unloading. The progressive loss of constraint is consistent with the absence of crack-initiation under type-I WPS. Evaluation of reloading effects associated with type-II and type-III WPS indicates that for a given state of reloading as characterized by the reload ratio K/K_{WPS}, the degree of crack-tip-constraint relaxation at $r / (J/\sigma_o)$ varies inversely with the extent of prior unloading. The inverse relationship is qualitatively consistent with the experimental observation of decrease in WPS-induced toughness with increase in the amount of unloading during the WPS cycle. The nature of the constraint effects under unloading and reloading corresponds to a spatially varying hydrostatic stress field relative to K-dominant SSY conditions in a manner somewhat similar to that associated with the Q-stress parameter. The range of WPS conditions under which a global measure of the crack-driving force in terms of K can be used to uniquely describe the crack-tip conditions are identified.

REFERENCES

[1] D. K. M. Shum, Martin Marietta Energy Systems, Inc., Oak Ridge Natl. Lab., *Preliminary Investigation on the Inclusion of Warm Prestress Effects in Fracture-Margin Assessment of Reactor Pressure Vessels*, USNRC Report NUREG/CR-5946 (ORNL/TM-12236), to be published.

[2] N. P. O'Dowd, C. F. Shih, *Two-Parameter Fracture Mechanics: Theory and Applications*, USNRC Report NUREG/CR-5958 (CDNSWC/SME-CR-16-92), February 1993.

[3] D. K. M. Shum, Martin Marietta Energy Systems, Inc., Oak Ridge Natl. Lab., *Implications of Warm Prestress on Safety-Margin Assessment of Reactor Pressure Vessels*, USNRC Letter Report ORNL/NRC/LTR-91/9, May 1992.

[4] United States Nuclear Regulatory Commission. *Regulatory Guide 1.154*, "Format and Content of Plant-Specific Pressurized Thermal Shock Safety Analysis Reports for Pressurized Water Reactors," January 1987.

[5] D. J. Naus et al., Martin Marietta Energy Systems, Inc., Oak Ridge Natl. Lab., *Crack-Arrest Behavior in SEN Wide Plates of Quenched and Tempered A533 Grade B Steel Tested Under Nonisothermal Conditions*, USNRC Report NUREG/CR-4930 (ORNL-6388), August 1987.

[6] R.B. Stonesifer, E.F. Rybicki and D.E. McCabe, *Warm Prestress Modeling: Comparison of Models and Experimental Results*, USNRC Report NUREG/CR-5208 (MEA-2305), April 1989.

[7] Abaqus *User Manual*, Version 4-9-1, Hibbit, Karlsson & Sorensen, Inc., Providence, Rhode Island, 1991.

[8] M. F. Kanninen and C. H. Popelar, Chapter 8 of *Advanced Fracture Mechanics*, Oxford University Press, New York, pp. 498-532, 1985.

[9] T. J. Theiss, D. K. M. Shum, S. T. Rolfe, Martin Marietta Energy Systems, Inc., Oak Ridge Natl. Lab., *Experimental and Analytical Investigation of the Shallow-Flaw Effect in Reactor Pressure Vessels*, USNRC Report NUREG/CR-5886 (ORNL/TM-12115), July 1992.

[10] A. G. Varias and C. F. Shih, "Quasi-Static Crack Advance Under a Range of Constraints - Steady-State Fields Based on a Characteristic Length", Division of Engineering, Brown University, June 1992.

[11] D. E. McCabe and R. K. Nanstad, "Effects of Cyclic Straining on Irradiation-Hardened Steel," Chapter 3 of *HSST Semiannual Progress Report for October 1990 - March 1991*, USNRC Report NUREG/CR-4219 (ORNL/TM-9593/V9&N1), pp. 25-26, November 1992.

DATE
FILMED
9/8/93
END